

TUNING OF FUZZY SHARPENING FILTERS FOR BIOMEDICAL IMAGE ENHANCEMENT

Jaromir Kukal^{1*}, Abduljalil Sireis², Zuzana Krbcova²

¹Czech Technical University in Prague
Faculty of Nuclear Sciences and Physical Engineering
Department of Software Engineering
Trojanova 13, 120 00 Prague 2
Czech Republic
jaromir.kukal@jfifi.cvut.cz

²University of Chemistry and Technology in Prague
Faculty of Chemical Engineering
Department of Computing and Control Engineering
Technicka 5, 166 26 Prague 6
Czech Republic

Abstract: Various approaches are used for image smoothing and sharpening. The class of fuzzy filters is widely used in the case of spiky noise due to their non-linear behavior. A lot of popular fuzzy filters are realizable in Lukasiewicz algebra with square root. Frequently applied low-pass fuzzy filters were selected from literature and used for the image sharpening with dyadic weights. The first aim of the paper is to find the optimum sharpening with the best Signal-to-Noise Ratio criterion for various noise types and offer general suggestions for fuzzy filter selection. Our results are directly applicable to tomographic images from MRI, PET and SPECT scanners.

Keywords: image smoothing, image sharpening, Lukasiewicz algebra, fuzzy image processing, filter bank, MRI, PET, SPECT

1 Introduction

There are many approaches for designing linear and nonlinear 2D image enhancement. As typical for biomedical SPECT, PET, and MRI scans, the spiky noise has to be eliminated by statistically robust filters. The paper is based on fuzzy image processing in Lukasiewicz algebra with square root [1, 2] which enables to realize robust low-pass and sharpening filters. The enhancement quality is measured by Signal to Noise Ratio (SNR) and various combinations of integer masks and sharpening approaches are applied to biomedical image with Gaussian and spiky noise. There is only a finite number of combinations and the most suitable ones are discussed.

Lukasiewicz algebra with square root is remembered in the second section. The next section summarizes several operations which are useful for data processing. The frame of fuzzy local image processing and computer experiment design are established in the fourth section. The fifth section summarizes the main results of optimal sharpening with the highest possible SNR [3] which is followed by concluding remarks.

2 Lukasiewicz Algebra with Square Root

The main idea behind the scope of the paper is to compare real properties of various fuzzy filters. First, it is necessary to specify the collection of permitted operations. Supposing intensity normalization into $[0, 1]$ interval, we decide to apply Many-Valued Algebra (MVA) [4]. Let $\mathcal{L} = [0, 1]$ be supporting set. The *Lukasiewicz algebra with square root* [2] is defined as

$$LA_{\text{sqrt}} = \langle \mathcal{L}, \wedge, \vee, \otimes, \rightarrow, 0, 1, \text{sqrt} \rangle \quad (1)$$

where

- $a \wedge b = \min(a, b)$,
- $a \vee b = \max(a, b)$,
- $0 = \min \mathcal{L}$,

- $1 = \max \mathcal{L}$,
- $a \otimes b = \max(a + b - 1, 0)$,
- $a \rightarrow b = \min(1 - a + b, 1)$,
- $\text{sqrt}(a) = \sqrt{a} = (1 + a)/2$.

Derived operators of LA_{sqrt} are

- $\neg a = 1 - a$,
- $a \oplus b = \neg(\neg a \otimes \neg b) = \min(a + b, 1)$,
- $a \ominus b = a \otimes \neg b = \max(a - b, 0)$.

Given algebra is frequently used in fuzzy image processing [5].

3 Permitted Operations in LA_{sqrt}

The main question is how to design selected operations for signal and image processing in given algebra. Fortunately, LA_{sqrt} is able to realize both traditional operators [5] and constrained linear transforms with dyadic weights. Let $a, b, c \in [0, 1]$ be fuzzy variables, k be order in sorted list of n values, $H \in \mathbb{N}_0$ be dyadic exponent, and $\alpha = m/2^N$ be dyadic weight. There are several cases:

- When $a + b \leq 1$, standard addition is realizable as $a + b = a \oplus b$.
- When $a \geq b$, standard subtraction is realizable as $a - b = a \ominus b$.
- Using functions $\varphi(x) = \text{sqrt}(x) \ominus (1/2) = x/2$ and $\text{trim}(x) = \min(1, \max(0, x))$ we can realize operations based on traditional multiplication by dyadic weight.

The last case can be proven as follows. First, $x/2^H = \varphi^{[H]}(x)$ where $\varphi^{[0]}(x) = x$, $\varphi^{[H]}(x) = \varphi(\varphi^{[H-1]}(x))$. Therefore, for $m \cdot x \leq 2^N$ we directly have

$$\frac{m \cdot x}{2^H} = \bigoplus_{k=1}^m \varphi^{[H]}(x) \tag{2}$$

which will be useful for realization of several linear filters.

Traditional image sharpening is unconstrained and based on formula $a + \alpha \cdot (b - c)$ which has to be trimmed into $[0, 1]$ interval in the case of fuzzy processing. Therefore, we directly calculate

$$\text{trim}(a + \alpha \cdot (b - c)) = a \oplus \alpha \cdot (b \ominus c) \ominus \alpha \cdot (c \ominus b). \tag{3}$$

Finally, when the data list of n values is sorted as

$$x_{(1)} \leq x_{(2)} \leq \dots \leq x_{(n)} \tag{4}$$

the k^{th} value $x_{(k)}$ can be expressed in Disjoint Normal Form (DNF) and directly calculated using operators \vee, \wedge .

4 Fuzzy Local Image Processing

Using simple tricks from previous section, we can perform selected procedures of local image processing. Basic terms and operations are recalled first. Let $M, N \in \mathbb{N}$ be height and width of normalized image $\mathbf{X} \in [0, 1]^{M \times N}$. The local image processing operates on list of values [6] from pixel neighborhood. The values are represented by vector $\mathbf{x} \in [0, 1]^m$ of length $m \in \mathbb{N}$. It can be connected with vector $\mathbf{y} \in [0, 1]^n$ of length $n \in \mathbb{N}$ using operator

$$\mathbf{x} \sqcup \mathbf{y} = (x_1, x_2, \dots, x_m, y_1, y_2, \dots, y_n)^T. \tag{5}$$

Aggregation operator [3] is therefore defined as

$$\bigsqcup_{k=1}^N \mathbf{x}_k = \mathbf{x}_1 \sqcup \mathbf{x}_2 \sqcup \dots \sqcup \mathbf{x}_n. \tag{6}$$

Multiple evidence of values can be obtained by multiplication operator

$$n \odot \mathbf{x} = \bigsqcup_{k=1}^N \mathbf{x} \tag{7}$$

which will be also useful for mask applications.

The integer mask of radius $r \in \mathbb{N}$ is represented by matrix $\mathbf{W} \in \mathbb{N}_0^{(2r+1) \times (2r+1)}$ with central symmetry. The local processing with mask \mathbf{W} of image part $\mathbf{B} \in [0, 1]^{(2r+1) \times (2r+1)}$ generates the weighted list of values [3] as vector

$$\mathbf{x} = \bigsqcup_{i=1}^{2r+1} \bigsqcup_{j=1}^{2r+1} (w_{i,j} \odot b_{i,j}) \tag{8}$$

of length n and any permitted operation from LA_{sqrt} can be used for local processing. The local fuzzy image processing is frequently based on the evaluation of sample statistics:

- *Erosion* [3] as $E(\mathbf{x}) = \bigwedge_{k=1}^n x_k$,
- *Dilation* [3] as $D(\mathbf{x}) = \bigvee_{k=1}^n x_k$,
- *Median* [7, 8] for odd n as $M(\mathbf{x}) = x_{(k)}$ where $k = (n + 1)/2$,
- *Median* for even n as $M(\mathbf{x}) = \varphi(x_{(k)}) \oplus \varphi(x_{(k+1)})$ where $k = n/2$,
- *First quartile* [9] as $Q_1(\mathbf{x}) = M(x_{(1)}, \dots, x_{(k)})$ where $k = \lfloor n/2 \rfloor$,
- *Third quartile* [9] as $Q_3(\mathbf{x}) = M(x_{(k)}, \dots, x_{(n)})$ where $k = \lceil n/2 \rceil + 1$,
- *Average* [10] for dyadic $n = 2^H$ as $A(\mathbf{x}) = \bigoplus_{k=1}^n \varphi^{[H]}(x_{(k)})$.

More sophisticated statistical calculations are based on *Walsh list* [11] which was originally published as

$$W(\mathbf{x}) = \bigsqcup_{i \leq j} \frac{x_i + x_j}{2} \tag{9}$$

but can be expressed in fuzzy form

$$W(\mathbf{x}) = \bigsqcup_{i=1}^n \bigsqcup_{j=i}^n (\varphi(x_i) \oplus \varphi(x_j)). \tag{10}$$

The other useful local operators are [3]:

- *Hodges–Lehmann Median* [11] as $H(\mathbf{x}) = M(W(\mathbf{x}))$,
- *Opening* $O(\mathbf{x})$ as erosion followed by dilation,
- *Closing* $C(\mathbf{x})$ as dilation followed by erosion,
- *OC Mean* $OCM(\mathbf{x}) = \varphi(O(\mathbf{x})) \oplus \varphi(C(\mathbf{x}))$,
- *OC Filter* $OC(\mathbf{x})$ as opening followed by closing,
- *CO Filter* $CO(\mathbf{x})$ as closing followed by opening,
- *OCCO Mean* $OCCOM(\mathbf{x}) = \varphi(OC(\mathbf{x})) \oplus \varphi(CO(\mathbf{x}))$,
- *Constrained Filter* $CF(\mathbf{x}) = (A(\mathbf{x}) \vee Q_1(\mathbf{x})) \wedge Q_3(\mathbf{x})$ and the central weight of mask \mathbf{W} needs to be replaced by zero.

Previous approaches can be used for *Fuzzy Low-Pass* (FLP) [12] filtering which should improve the image quality. Another possibility is to apply FLP filter in image sharpening process using x_c as intensity behind the mask center. Resulted sharpening operator

$$S(\mathbf{x}) = \text{FLP}(\mathbf{x}) + \alpha \cdot (x_c - \text{FLP}(\mathbf{x})) \tag{11}$$

is also realizable in $\text{LA}_{\text{sqr}}t$ for dyadic sharpening gain $\alpha \geq 0$.

5 Sharpening Filters Portfolio

Various low-pass fuzzy filters with various but symmetric masks will be used for image sharpening with dyadic gain. Resulting bank of fuzzy filters is determined by filtering approaches and mask weights.

5.1 Fuzzy Filtering Approaches

Various fuzzy sharpening approaches were used for 2D image enhancement. List of fuzzy low-pass filters is included in Tab. 1. Image sharpening gain was studied for $\alpha \in \{k/32 : k = 0, \dots, 160\}$ for various images and noise types.

Table 1: Low-Pass Filter Portfolio

Index	Filter	Description
1	M	Median
2	A	Average
3	H	Hodges-Lehmann
4	O	Opening
5	C	Closing
6	OCM	Opening-Closing Mean
7	OC	Opening followed by Closing
8	CO	Closing followed by Opening
9	OCCOM	OC and CO Mean
10	CF	Constrained Filter

5.2 Compact 3×3 Masks

In this study we used five small compact masks as

$$\mathbf{M}_1 = \begin{pmatrix} 0 & 1 & 0 \\ 1 & 1 & 1 \\ 0 & 1 & 0 \end{pmatrix}, \mathbf{M}_2 = \begin{pmatrix} 0 & 1 & 0 \\ 1 & 4 & 1 \\ 0 & 1 & 0 \end{pmatrix},$$

$$\mathbf{M}_3 = \begin{pmatrix} 1 & 1 & 1 \\ 1 & 1 & 1 \\ 1 & 1 & 1 \end{pmatrix}, \mathbf{M}_4 = \begin{pmatrix} 1 & 1 & 1 \\ 1 & 8 & 1 \\ 1 & 1 & 1 \end{pmatrix}, \mathbf{M}_5 = \begin{pmatrix} 1 & 2 & 1 \\ 2 & 4 & 2 \\ 1 & 2 & 1 \end{pmatrix}$$

but only $\mathbf{M}_2, \mathbf{M}_4, \mathbf{M}_5$ are applicable in average filter.

5.3 Compact 5×5 Masks

Seven large compact masks were also used as

$$\mathbf{M}_6 = \begin{pmatrix} 0 & 0 & 1 & 0 & 0 \\ 0 & 1 & 1 & 1 & 0 \\ 1 & 1 & 1 & 1 & 1 \\ 0 & 1 & 1 & 1 & 0 \\ 0 & 0 & 1 & 0 & 0 \end{pmatrix}, \mathbf{M}_7 = \begin{pmatrix} 0 & 0 & 1 & 0 & 0 \\ 0 & 1 & 1 & 1 & 0 \\ 1 & 1 & 4 & 1 & 1 \\ 0 & 1 & 1 & 1 & 0 \\ 0 & 0 & 1 & 0 & 0 \end{pmatrix},$$

$$\mathbf{M}_8 = \begin{pmatrix} 0 & 1 & 1 & 1 & 0 \\ 1 & 1 & 1 & 1 & 1 \\ 1 & 1 & 1 & 1 & 1 \\ 1 & 1 & 1 & 1 & 1 \\ 0 & 1 & 1 & 1 & 0 \end{pmatrix}, \mathbf{M}_9 = \begin{pmatrix} 0 & 1 & 1 & 1 & 0 \\ 1 & 1 & 1 & 1 & 1 \\ 1 & 1 & 12 & 1 & 1 \\ 1 & 1 & 1 & 1 & 1 \\ 0 & 1 & 1 & 1 & 0 \end{pmatrix},$$

$$\mathbf{M}_{10} = \begin{pmatrix} 1 & 1 & 1 & 1 & 1 \\ 1 & 1 & 1 & 1 & 1 \\ 1 & 1 & 1 & 1 & 1 \\ 1 & 1 & 1 & 1 & 1 \\ 1 & 1 & 1 & 1 & 1 \end{pmatrix}, \mathbf{M}_{11} = \begin{pmatrix} 1 & 1 & 1 & 1 & 1 \\ 1 & 1 & 1 & 1 & 1 \\ 1 & 1 & 8 & 1 & 1 \\ 1 & 1 & 1 & 1 & 1 \\ 1 & 1 & 1 & 1 & 1 \end{pmatrix},$$

$$\mathbf{M}_{12} = \begin{pmatrix} 1 & 4 & 6 & 4 & 1 \\ 4 & 16 & 24 & 16 & 4 \\ 6 & 24 & 36 & 24 & 6 \\ 4 & 16 & 24 & 16 & 4 \\ 1 & 4 & 6 & 4 & 1 \end{pmatrix}$$

but only $\mathbf{M}_7, \mathbf{M}_9, \mathbf{M}_{11}, \mathbf{M}_{12}$ are applicable in average filter.

5.4 Ring Masks

The dyadic property was also obtained by removing central points. Resulting ring masks are

$$\mathbf{M}_{13} = \begin{pmatrix} 0 & 1 & 0 \\ 1 & 0 & 1 \\ 0 & 1 & 0 \end{pmatrix}, \mathbf{M}_{14} = \begin{pmatrix} 1 & 1 & 1 \\ 1 & 0 & 1 \\ 1 & 1 & 1 \end{pmatrix},$$

$$\mathbf{M}_{15} = \begin{pmatrix} 0 & 0 & 1 & 0 & 0 \\ 0 & 1 & 0 & 1 & 0 \\ 1 & 0 & 0 & 0 & 1 \\ 0 & 1 & 0 & 1 & 0 \\ 0 & 0 & 1 & 0 & 0 \end{pmatrix}, \mathbf{M}_{16} = \begin{pmatrix} 0 & 1 & 1 & 1 & 0 \\ 1 & 1 & 0 & 1 & 1 \\ 1 & 0 & 0 & 0 & 1 \\ 1 & 1 & 0 & 1 & 1 \\ 0 & 1 & 1 & 1 & 0 \end{pmatrix}.$$

6 Optimal Sharpening in $LA_{\text{sqr}}t$

Numerical experiments on two representative images were performed to obtain the best possible increasing of Signal to Noise Ratio (SNR) as generally recommended criterion. Pixel intensity of ideal image was normalized into interval $[0, 1]$, first. The random noise was added and resulting image was constrained to original range $[0, 1]$ as model of real image in the second step. Various types of fuzzy sharpening filters with various masks and sharpening gains were applied to real image to obtain a set of enhanced images.

The *SNR* criterion was designed using the logarithmic scale as

$$SNR = 10 \log_{10} \left(\frac{P_{\text{signal}}}{P_{\text{noise}}} \right) \tag{12}$$

where $P_{\text{signal}}, P_{\text{noise}}$ are average powers of the signal and additive noise. The quality of sharpening was studied as improvement $\Delta SNR = SNR - SNR_0$ in dB where SNR_0, SNR reflect the image quality before and after the sharpening.

A slice of human brain 2D MRI ROI of size 40×40 was used in the first case together with additive Gaussian noise $\sigma = 0.05$ as example of low-level noise. Results of sharpening are included in Tabs. 2,3 as optimal increasing of SNR value and adequate sharpening gain. The symbol * means that the filter cannot be realized in the fuzzy system. The best results were obtained for averaging filter F_2 with four-point ring mask \mathbf{M}_{13} . The same mask also produced acceptable increasing of SNR for Hodges–Lehmann median F_3 , median F_1 , and constrained filter F_{10} with $\alpha = 13/32$ in majority of cases. The open–closing filter F_6 is also acceptable with five-point mask \mathbf{M}_1 and $\alpha = 1/16$. The noised MRI image and the result of the best filter F_2 are depicted in Fig. 1.

The same image of size 40×40 was used in the second case with spiky noise generated as follows. Additive Gaussian noise with $\sigma = 0.1$ was corrupted by pepper-salt noise with probability 0.05. Results of sharpening are included in Tabs. 4,5 as optimal SNR increasing values and adequate sharpening gains. The best results were obtained for Hodges–Lehmann median filter F_3 with binomial mask \mathbf{M}_{12} and $\alpha = 0$. The median F_1 , OCCOM F_9 , and constrained F_{10} filters over–performed the average filter F_2 in SNR improvement. The same MRI image corrupted by spiky noise and the result of the best filter F_3 are depicted in Fig. 1.

7 Conclusions

The fuzzy low–pass and sharpening filters have been investigated in the case of MRI images with Gaussian and spiky noise. The best results in ΔSNR were obtained for Hodges–Lehmann low–pass filter with binomial 5×5

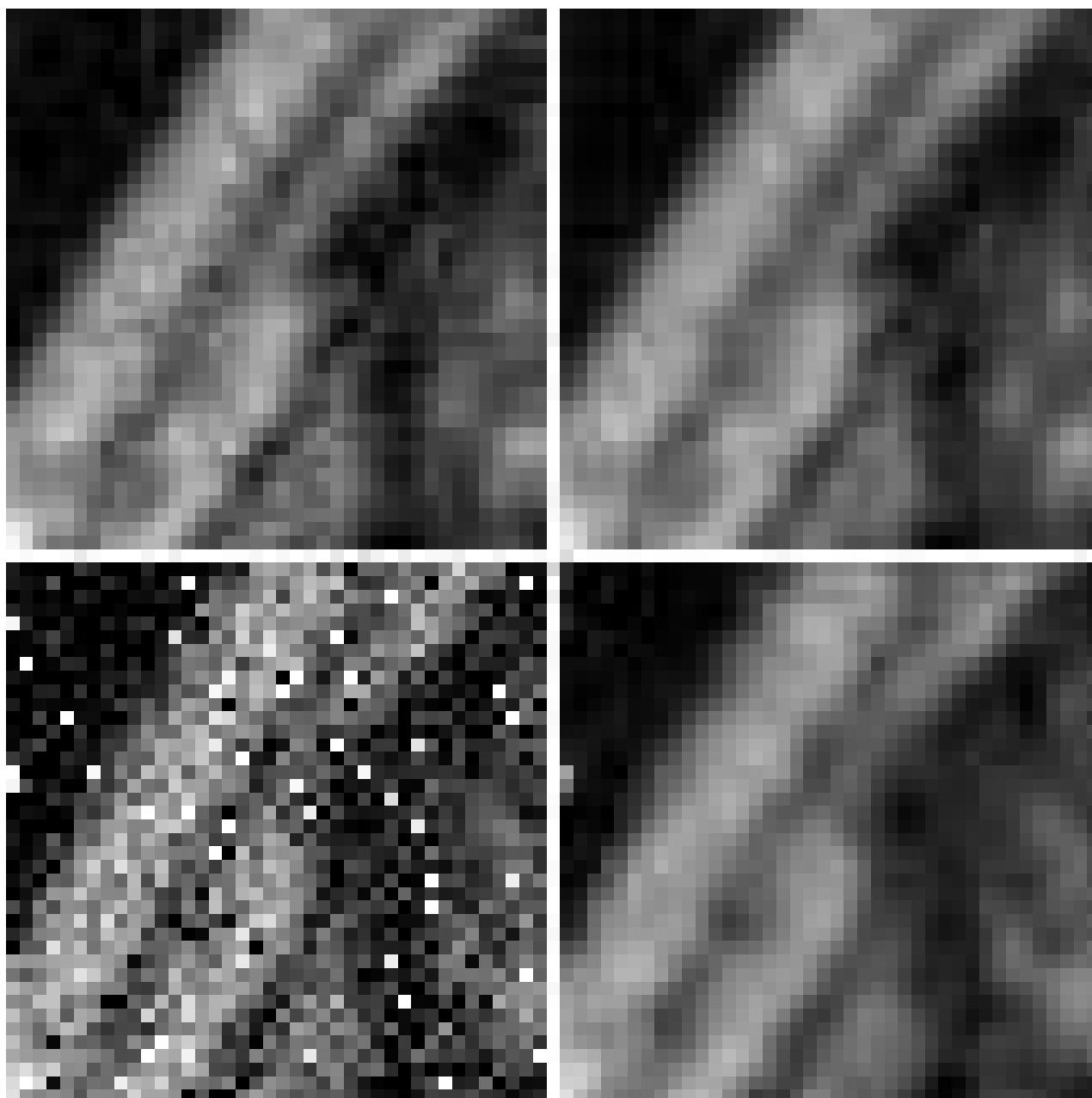


Figure 1: Performance of fuzzy filters: Gaussian-noised image (left top), smoothing by dyadic average (right top), spiky-noised image (left bottom), smoothing by Hodges-Lehmann median (bottom right)

mask in the case of pepper-salt noise. The same filtering approach was also suitable in the case of Gaussian noise however the best choice is dyadic average low-pass filter with four-point ring 3×3 mask in the Gaussian case. This study can be useful for future biomedical applications with unknown noise type and range when the Hodges-Lehmann low-pass filter with binomial 5×5 mask frequently overperforms traditional linear, median, and morphological filters and the sharpening is omitted.

Acknowledgement: This paper is supported by SGS17/196/OHK4/3T/14 grant of Czech Technical University in Prague, grant GA17-05840S of the Czech Science Foundation, and MSMT No 21-SVV/2018.

References

- [1] Hajek, P.: *Metamathematics of Fuzzy Logic*. Kluwer, Dordrecht (1998)
- [2] Novak, V., Perfilieva, I., Mockor, J.: *Mathematical Principles of Fuzzy Logic*. Kluwer Academic Publishers, Boston (1999)
- [3] Gonzalez, R.C., Woods, R.E.: *Digital Image Processing (3rd edition)*. Prentice Hall, New York (2008)

Table 2: Sharpening quality as ΔSNR [dB] for Gaussian noise

MASK	F ₁	F ₂	F ₃	F ₄	F ₅	F ₆	F ₇	F ₈	F ₉	F ₁₀
1	1.37	*	1.71	0.66	0.42	1.18	0.76	0.67	0.86	*
2	0.43	1.78	1.24	0.66	0.42	1.18	0.76	0.67	0.86	1.77
3	1.51	*	1.66	0.46	0.21	0.75	0.40	0.25	0.43	*
4	0.21	1.53	1.26	0.46	0.21	0.75	0.40	0.25	0.43	1.50
5	1.35	1.69	1.73	0.46	0.21	0.75	0.40	0.25	0.43	1.68
6	1.13	*	1.07	0.29	0.13	0.47	0.23	0.14	0.24	*
7	0.89	0.94	1.12	0.29	0.13	0.47	0.23	0.14	0.24	0.94
8	0.86	*	0.67	0.18	0.09	0.33	0.14	0.08	0.15	*
9	0.39	0.54	0.77	0.18	0.09	0.33	0.14	0.08	0.15	0.55
10	0.74	*	0.54	0.13	0.03	0.19	0.09	0.03	0.08	*
11	0.55	0.41	0.62	0.13	0.03	0.19	0.09	0.03	0.08	0.41
12	1.24	1.04	1.25	0.13	0.03	0.19	0.09	0.03	0.08	1.04
13	1.67	1.85	1.79	0.54	0.31	0.90	0.57	0.48	0.61	1.85
14	1.65	1.55	1.66	0.43	0.20	0.69	0.41	0.29	0.44	1.55
15	0.81	0.58	0.63	0.21	0.09	0.09	0.18	0.12	0.19	0.58
16	0.63	0.36	0.42	0.17	0.09	0.09	0.14	0.09	0.15	0.36

Table 3: Sharpening gain α (in 1/32) for Gaussian noise

MASK	F ₁	F ₂	F ₃	F ₄	F ₅	F ₆	F ₇	F ₈	F ₉	F ₁₀
1	9	*	8	16	19	2	17	18	14	*
2	0	0	0	16	19	2	17	18	14	0
3	11	*	11	22	25	13	23	25	22	*
4	0	0	0	22	25	13	23	25	22	1
5	5	7	6	22	25	13	23	25	22	8
6	15	*	16	26	28	20	27	28	26	*
7	9	14	11	26	28	20	27	28	26	14
8	19	*	21	28	29	23	28	29	28	*
9	7	17	10	28	29	23	28	29	28	17
10	20	*	22	29	30	26	29	31	29	*
11	15	22	18	29	30	26	29	31	29	22
12	12	16	13	29	30	26	29	31	29	16
13	14	13	13	17	21	6	19	20	18	13
14	14	14	14	22	25	14	23	24	21	14
15	21	22	22	27	28	28	27	28	27	22
16	22	25	24	28	29	29	28	29	28	25

[4] Azevedo, F.: Constraint Solving over Multi-Valued Logics: Application to Digital Circuits. IOS Press, New York (2003)

[5] Majerova, D.: Image Processing by Means of Lukasiewicz Algebra with Square Root. PhD Thesis, ICT Prague (2004)

[6] Wasserman, S., Faust, K.: Social Network Analysis: Methods and Applications (2nd edition). Cambridge University Press, New York (2006)

[7] Arce, G.R.: Nonlinear Signal Processing: A Statistical Approach. Wiley, New Jersey (2005)

[8] Arias-Castro, E., Donoho, D.L.: Does Median Filtering Truly Preserve Edges Better than Linear Filtering. *Annals of Statistics* **37**(3), 1172-1196 (2009)

[9] Hyndman, R.J., Fan, Y.: Sample Quantiles in Statistical Packages. *American Statistician* **50**(4), 361-365 (1996)

[10] Hall, M.: Smooth Operator: Smoothing Seismic Horizons and Attributes. *The Leading Edge* **26**(1), 16-20 (2007)

[11] Hodges, J.L., Lehmann, E.L.: Estimates of Location Based on Rank Tests. *The Annals of Mathematical Statistics* **34**(2), 598-611 (1963)

[12] Mitra, S.K., Kaiser, J.F.: Handbook for Digital Signal Processing. John Wiley, New York (1993)

Table 4: Sharpening quality as ΔSNR [dB] for spiky noise

MASK	F ₁	F ₂	F ₃	F ₄	F ₅	F ₆	F ₇	F ₈	F ₉	F ₁₀
1	6.67	*	7.39	3.95	0.93	5.15	6.28	6.00	8.09	*
2	2.42	4.40	4.13	3.95	0.93	5.15	6.28	6.00	8.09	6.33
3	8.38	*	8.51	3.13	0.63	4.64	4.73	3.60	6.84	*
4	1.85	4.71	4.57	3.13	0.63	4.64	4.73	3.60	6.84	7.34
5	7.08	6.66	8.08	3.13	0.63	4.64	4.73	3.60	6.84	7.37
6	8.23	*	8.26	2.88	0.61	4.67	4.14	3.31	6.36	*
7	7.48	6.18	7.76	2.88	0.61	4.67	4.14	3.31	6.36	7.32
8	7.99	*	7.93	2.09	0.43	3.55	2.96	2.23	5.34	*
9	5.13	5.60	5.42	2.09	0.43	3.55	2.96	2.23	5.34	7.07
10	7.70	*	7.60	1.71	0.37	3.15	2.26	1.79	4.56	*
11	7.36	6.19	7.03	1.71	0.37	3.15	2.26	1.79	4.56	6.95
12	8.55	7.17	8.61	1.71	0.37	3.15	2.26	1.79	4.56	7.41
13	7.21	5.80	7.25	3.74	0.73	4.54	6.07	5.75	7.37	5.80
14	8.56	6.94	8.34	3.48	0.80	5.12	5.36	4.92	7.32	7.08
15	7.24	5.95	7.16	3.23	1.02	5.01	4.83	4.16	6.25	6.04
16	7.10	6.10	7.07	2.69	0.91	5.07	3.96	3.44	5.98	6.20

Table 5: Sharpening gain α (in 1/32) for spiky noise

MASK	F ₁	F ₂	F ₃	F ₄	F ₅	F ₆	F ₇	F ₈	F ₉	F ₁₀
1	0	*	0	6	11	0	4	2	0	*
2	0	0	0	6	11	0	4	2	0	0
3	1	*	1	11	20	0	8	9	2	*
4	0	0	0	11	20	0	8	9	2	0
5	0	0	0	11	20	0	8	9	2	0
6	2	*	1	13	21	0	10	11	3	*
7	0	0	0	13	21	0	10	11	3	0
8	2	*	2	17	25	4	15	16	6	*
9	0	0	0	17	25	4	15	16	6	0
10	3	*	3	20	26	6	18	18	8	*
11	0	0	0	20	26	6	18	18	8	0
12	0	0	0	20	26	6	18	18	8	0
13	4	7	4	6	14	0	3	2	0	7
14	3	5	3	9	16	0	6	5	1	5
15	4	6	4	10	15	0	8	8	3	6
16	4	5	4	14	19	0	11	11	5	5